

The University of Reading

Data Assimilation for Parameter
Estimation with Application to a Simple
Morphodynamic Model

P.J. Smith¹, M.J. Baines¹, S.L. Dance¹, N.K. Nichols¹ and
T.R. Scott²

MATHEMATICS REPORT 2/2008

¹ <i>Department of Mathematics</i>	² <i>Environmental Systems Science Centre</i>
<i>The University of Reading</i>	<i>The University of Reading</i>
<i>Whiteknights, PO Box 220</i>	<i>Earley Gate,</i>
<i>Reading, RG6 6AX</i>	<i>Reading, RG6 6AL</i>

Department of Mathematics

Data Assimilation for Parameter Estimation with Application to a Simple Morphodynamic Model

P.J. Smith, M.J. Baines, S.L. Dance, N.K. Nichols, T.R. Scott

August 2008

Abstract

Data assimilation is a means for combining observational data with model predictions to produce state and parameter estimates that most accurately approximate the current and future states of the true system. The technique is commonly used in atmospheric and oceanic modelling, combining empirical observations with model predictions to produce more accurate and well-calibrated forecasts. Here we consider its application within a coastal environment and describe how the method can also be used to deliver improved estimates of uncertain morphodynamic model parameters. This is achieved using a technique known as state augmentation. A simple 1D model of bed-form propagation is used to demonstrate the method within a three dimensional variational assimilation framework. Preliminary results are positive and suggest the potential for application to more complex morphodynamic models.

1 Introduction

Changes to weather patterns, with increasing incidence of coastal flooding in recent years, have led to growing concern over the effects of climate change on flooding and highlighted the importance of accurate knowledge of coastal morphology in natural disaster prediction and management. It is essential that we improve our ability to predict floods; being able to better identify and anticipate flood risk would facilitate the development of suitable strategies for the management of coastal areas and help to limit the damage and distress caused by flooding. Key to this is better knowledge and understanding of how the morphology of the coastal zone is evolving over time [Nicholls et al. (2007), Stelling (2000)]. Accurate bathymetry immediately prior to a storm event would allow improved flood forecasting using coastal inundation models.

Coastal morphodynamics presents a challenge to modellers. Modelling is difficult because longer term morphological changes are driven by shorter term processes such as waves and tides [Masselink and Hughes (2003)]. State of the art models are growing more sophisticated in an attempt to accurately model coastal morphology [e.g. Lesser et al. (2004)]. In practice, models suffer from uncertainty in their initial conditions and parameters which can lead to significant errors between the predicted and actual states of the system, so that coastal area morphodynamic models often perform poorly in detail. A complementary approach to improving model performance is to combine model integrations with observations of morphology using data assimilation techniques.

Data assimilation is a means for combining observational data with model predictions to 1) produce a model state that most accurately approximates the current and future states of the true system 2) provide estimates of the model parameters. It is routinely used in atmospheric and oceanic prediction, but the possibility of transferring the technique into the coastal environment has only recently been investigated [Scott and Mason (2007)]. The overall aim of this work is to apply data assimilation within a coastal morphodynamic model, exploiting the information content of empirical observations to give more accurate and well calibrated forecasts. In this study we focus

on the second of these applications and describe a method for using data assimilation to deliver improved parameter estimates.

The dynamical system we wish to model depends on parameters whose exact values are not known, for example those that arise from parameterization of the sediment transport flux. Inaccurate representation of model parameters can lead to the growth of model error and therefore effect the ability of our model to accurately predict the true system state. A key question in model development is how to estimate these values *a priori*. Generally, parameters are determined theoretically or by calibration of the model against observations. Here we present an alternative approach using a variational data assimilation technique within a simplified 1D model of bedform propagation to develop a scheme that enables model parameters to be estimated alongside the model bathymetry as part of the assimilation process.

In section 2 we present the data assimilation problem for a general case and give an overview of the three dimensional variational assimilation algorithm used in this work. In section 3 we describe the technique employed for parameter estimation and reformulate the data assimilation problem for this special case. Our simple 1D model is introduced in section 4. In section 5 we discuss the roles of the observation and background error covariance matrices. Particular attention is given to the cross correlations between the background errors in the state and parameter estimates. The experimental design is described in section 6 followed by results in section 7. Finally, in section 8 we summarise the conclusions from this work and outline areas for further study.

2 Data assimilation for state estimation

In reality, a model cannot represent the behaviour of a morphodynamic system exactly. Over time the model bathymetry will diverge from the true bathymetry and errors will arise due to imperfect initial conditions and inaccuracies in physical equations, parameters and numerical implementation. Data assimilation can be used to compensate for the inadequacies of a model and help keep the model bathymetry on track. By periodically incorporating measured observations into the model, data assimilation nudges the model bathymetry back towards the true bathymetry, thus improving the ability of the model to predict future bathymetry.

In this report we consider the discrete, linear, time-invariant system model

$$\mathbf{z}_{k+1} = M\mathbf{z}_k, \quad k = 0, \dots, N - 1, \quad (2.1)$$

where the vector $\mathbf{z}_k \in \mathbb{R}^m$ represents the model state at time t_k and $M \in \mathbb{R}^{m \times m}$ is a constant, non-singular matrix describing the dynamic evolution of the state from time t_k to time t_{k+1} .

We have a set of r observations to assimilate and these are related to the model state by the equations

$$\mathbf{y}_k = \mathbf{h}(\mathbf{z}_k) + \boldsymbol{\varepsilon}_k^o, \quad k = 0, \dots, N - 1, \quad (2.2)$$

where $\mathbf{y}_k \in \mathbb{R}^r$ is a vector of r observations at time t_k , $\mathbf{h} : \mathbb{R}^m \rightarrow \mathbb{R}^r$ is a nonlinear observation operator that maps from model to observation space, and $\boldsymbol{\varepsilon}_k^o \in \mathbb{R}^r$ is a random vector representing the observation errors. If we have direct observations, \mathbf{h} is simply an interpolation operator for interpolating variables from the model grid to observation locations. Often, the model variables we wish to analyse cannot be observed directly and instead we have observations of another measurable quantity. In this case, \mathbf{h} will also include transformations based on physical relationships that convert the model variables to the observations. We also assume that an *a priori* or *background* estimate $\mathbf{z}_0^b \in \mathbb{R}^m$ of the initial system state \mathbf{z}_0 is known with error $\boldsymbol{\varepsilon}^b$.

The aim of data assimilation is to combine the measured observations \mathbf{y} with the model predictions \mathbf{z}^b to derive a model state $\mathbf{z}^a \in \mathbb{R}^m$ that most accurately describes the true state of the system \mathbf{z}^t . This optimal estimate is called the *analysis*.

A wide variety of data assimilation schemes exist, many of which have been derived using statistical techniques [e.g. Griffith (1997), Kalnay (2003)]. In this work we apply a standard method based on statistical estimation theory known as *three dimensional variational data assimilation* (3D Var). The prefix ‘3D’ refers to the fact that the method resolves the three spatial dimensions. The fourth dimension (time) is not accounted for; instead 3D Var schemes are designed to produce an analysis at a single time. Typically, observations are not taken simultaneously but are collected across a given time window. 3D Var schemes assume that the state does not evolve significantly within this period and treats all observations as if they had been taken at the same time. 3D Var is a robust and well established method that is relatively easy to implement and computationally efficient. Four dimensional variational data assimilation (4D Var) is an extension to the 3D Var technique that allows a complete time sequence of observations to be assimilated. Although more advanced, implementation of this method is complex and computationally expensive. We will not discuss the 4D Var algorithm further here, but note that details of its mathematical formulation can be found in the literature [e.g. Kalnay (2003), Nichols (2003)].

2.1 3D Variational assimilation

3D Var is based on a maximum a posteriori estimate approach and derives the analysis by looking for a state that minimises a cost function measuring the misfit between the model state \mathbf{z} and the background \mathbf{z}^b and observations \mathbf{y} ,

$$J(\mathbf{z}) = (\mathbf{z} - \mathbf{z}^b)^T \mathbf{B}^{-1} (\mathbf{z} - \mathbf{z}^b) + (\mathbf{y} - \mathbf{h}(\mathbf{z}))^T \mathbf{R}^{-1} (\mathbf{y} - \mathbf{h}(\mathbf{z})). \quad (2.3)$$

$\mathbf{B} \in \mathbb{R}^{m \times m}$ and $\mathbf{R} \in \mathbb{R}^{r \times r}$ are the covariance matrices of the background and observation errors. If we assume that the background and observation errors are unbiased, i.e.

$$E(\boldsymbol{\varepsilon}^b) = E(\boldsymbol{\varepsilon}^o) = 0,$$

where $\boldsymbol{\varepsilon}^b = \mathbf{z}^b - \mathbf{z}^t$ and $\boldsymbol{\varepsilon}^o = \mathbf{y} - \mathbf{h}(\mathbf{z}^t)$, we can define \mathbf{B} and \mathbf{R} as

$$\mathbf{B} = E\left(\boldsymbol{\varepsilon}^b (\boldsymbol{\varepsilon}^b)^T\right), \quad \mathbf{R} = E\left(\boldsymbol{\varepsilon}^o (\boldsymbol{\varepsilon}^o)^T\right). \quad (2.4)$$

These matrices represent the errors associated with the background and observations and determine the relative weighting of \mathbf{z}^b and \mathbf{y} in the analysis. If it is assumed that the background errors are small relative to the observation errors then the analysis is close to the background state. Conversely, if it is assumed that the background errors are relatively large the analysis will lie closer to the observations.

To determine the minimising state we use the gradient of the cost function with respect to \mathbf{z} . The analysis \mathbf{z}^a is then given by the solution of

$$\nabla J(\mathbf{z}^a) = 2\mathbf{B}^{-1}(\mathbf{z}^a - \mathbf{z}^b) - 2\mathbf{H}^T \mathbf{R}^{-1}(\mathbf{y} - \mathbf{h}(\mathbf{z}^a)) = 0. \quad (2.5)$$

∇J is known as the gradient vector, and the matrix $\mathbf{H} \in \mathbb{R}^{r \times m}$ represents the linearisation (Jacobian) of the observation operator \mathbf{h} .

Rearranging (2.5) gives us the following expression for the analysis

$$\mathbf{z}^a = \mathbf{z}^b + \mathbf{K}(\mathbf{y} - \mathbf{h}(\mathbf{z}^b)). \quad (2.6)$$

The operator $\mathbf{K} \in \mathbb{R}^{m \times r}$ is known as the gain matrix [Nichols (2003)] and is given by

$$\mathbf{K} = \mathbf{B}\mathbf{H}^T(\mathbf{H}\mathbf{B}\mathbf{H}^T + \mathbf{R})^{-1}. \quad (2.7)$$

This is the formal solution to the optimisation problem. Rather than calculating \mathbf{K} explicitly and solving the analysis equation (2.6), variational methods minimise the cost function (2.3) directly, using gradient methods to iterate to the minimising solution.

2.2 The assimilation algorithm

We apply our 3D Var data assimilation scheme sequentially. Each cycle of the algorithm can be split into two main phases which we outline below [Kalnay (2003)]:

1. The *forecast* phase in which the the analysis from the previous time step \mathbf{z}_k^a is integrated forward using the dynamic forecast model (2.1) to the time t_{k+1} when a set of observations become available. This predicted model state provides us with a background estimate of the true state \mathbf{z}_{k+1}^b . At the start of the first forecast phase an *a priori* estimate for the initial model state \mathbf{z}_0^b needs to be chosen.
2. The *analysis* phase in which the 3D Var cost function is mimimised iteratively through application of a suitable descent algorithm. This gives us a new analysis state \mathbf{z}_{k+1}^a ; this is an improved estimate of the current system state that can be used as the starting point for the next forecast step.

Once the analysis phase is complete we advance to the start of the next cycle and the process is repeated. The propagation of the previous analysis during the forecast phase means that information from past observations is retained and will therefore also have influence at subsequent analysis times.

3 State Augmentation

The equations used to describe the dynamical system we wish to model depend on parameters whose values are imprecisely known. Data assimilation provides us with a method for estimating these parameters using observational information. This can be achieved through *state augmentation*. State augmentation is a conceptually straightforward technique that allows us to estimate uncertain model parameters alongside the original model state [Jazwinski (1970)]. The approach has previously been used successfully in the context of model error estimation. Griffith and Nichols (1996) used the technique to develop a method for treating model error in Numerical Weather Prediction (NWP) as part of a variational data assimilation framework, and Martin (2000) explored the approach as a way of estimating systematic model errors in an oceanographic setting. Navon (1997) and Evensen et al. (1998) review the use of the technique in the context of 4D Var, and Dee (2005) reviews the use of a similar technique for bias estimation.

In theory, state augmentation can be applied to any of the standard data assimilation methods. The state vector is simply augmented with a vector containing the required parameters and the chosen assimilation algorithm is then applied to the augmented system in the usual way. In this study we consider application of the technique to parameter estimation using a 3D Var assimilation scheme.

3.1 Augmented data assimilation problem

We augment the state vector \mathbf{z} with a vector \mathbf{p} containing the parameters we wish to estimate, this gives us the *augmented state vector*

$$\mathbf{w} = \begin{pmatrix} \mathbf{z} \\ \mathbf{p} \end{pmatrix}, \quad (3.1)$$

where $\mathbf{z} \in \mathbb{R}^m$, $\mathbf{p} \in \mathbb{R}^q$, and $\mathbf{w} \in \mathbb{R}^{m+q}$.

We assume that the vector \mathbf{p} is constant; the parameters are not altered by the forecast model from one time step to the next and are only updated when a new 3D Var analysis is generated. We can therefore write the evolution model for the parameters as

$$\mathbf{p}_{k+1} = \mathbf{p}_k, \quad k = 0, \dots, N-1. \quad (3.2)$$

The system model then becomes

$$\begin{aligned} \mathbf{z}_{k+1} &= M(\mathbf{p}) \mathbf{z}_k \\ \mathbf{p}_{k+1} &= \mathbf{p}_k, \end{aligned}$$

which we can write as the equivalent augmented system

$$\mathbf{w}_{k+1} = \tilde{M} \mathbf{w}_k, \quad (3.3)$$

where

$$\tilde{M} = \begin{pmatrix} M(\mathbf{p}) & 0 \\ 0 & I \end{pmatrix} \in \mathbb{R}^{(m+q) \times (m+q)}.$$

Again, we assume we have observations given by

$$\mathbf{y} = \mathbf{h}(\mathbf{z}^t) + \boldsymbol{\varepsilon}_o, \quad \mathbf{y}, \boldsymbol{\varepsilon}_o \in \mathbb{R}^r.$$

We can write this in terms of the augmented state vector as

$$\mathbf{y} = \tilde{\mathbf{h}}(\mathbf{w}) + \boldsymbol{\varepsilon}_o, \quad (3.4)$$

where $\tilde{\mathbf{h}} : \mathbb{R}^{m+q} \rightarrow \mathbb{R}^r$, and

$$\tilde{\mathbf{h}}(\mathbf{w}) = \tilde{\mathbf{h}} \begin{pmatrix} \mathbf{z} \\ \mathbf{p} \end{pmatrix} = \mathbf{h}(\mathbf{z}).$$

The least squares cost function for the augmented state is the same as (2.3) but written in terms of the new variables

$$\tilde{J}(\mathbf{w}) = (\mathbf{w} - \mathbf{w}^b)^T \tilde{\mathbf{B}}^{-1} (\mathbf{w} - \mathbf{w}^b) + (\mathbf{y} - \tilde{\mathbf{h}}(\mathbf{w}))^T \mathbf{R}^{-1} (\mathbf{y} - \tilde{\mathbf{h}}(\mathbf{w})), \quad (3.5)$$

where

$$\mathbf{w}^b = \begin{pmatrix} \mathbf{z}^b \\ \mathbf{p}^b \end{pmatrix} \in \mathbb{R}^{m+q}, \quad (3.6)$$

is our background state. Note that this vector must now also include prior estimates of the parameters \mathbf{p}^b . These could be, for example, the latest estimates obtained from a previous analysis.

The matrix $\tilde{\mathbf{B}} \in \mathbb{R}^{(m+q) \times (m+q)}$ is the background error covariance matrix for the augmented system, and can be written as

$$\tilde{\mathbf{B}} = \begin{pmatrix} \mathbf{B}_{zz} & \mathbf{B}_{zp} \\ \mathbf{B}_{zp}^T & \mathbf{B}_{pp} \end{pmatrix}. \quad (3.7)$$

Here $\mathbf{B}_{zz} \in \mathbb{R}^{m \times m}$ is the covariance matrix of the background errors in the state estimate \mathbf{z}^b (defined as in (2.4)). $\mathbf{B}_{pp} \in \mathbb{R}^{q \times q}$ is the covariance matrix of the errors in the parameter vector \mathbf{p}^b and $\mathbf{B}_{zp} \in \mathbb{R}^{m \times q}$ is the covariance matrix for the cross correlations between the background errors in the state and parameter vectors. If we assume that the parameter errors are also unbiased, we can define

$$\mathbf{B}_{pp} = E(\boldsymbol{\varepsilon}_p \boldsymbol{\varepsilon}_p^T) \quad \text{and} \quad \mathbf{B}_{zp} = E(\boldsymbol{\varepsilon}_b \boldsymbol{\varepsilon}_p^T), \quad (3.8)$$

where $\boldsymbol{\varepsilon}_p = \mathbf{p}^b - \mathbf{p}^t$ and $\boldsymbol{\varepsilon}_b = \mathbf{z}^b - \mathbf{z}^t$.

Since they depend on the same data, we expect the errors in \mathbf{p}^b to be correlated with the background state estimation errors. Hence it is important that we do not neglect the matrix \mathbf{B}_{zp} .

The augmented gradient vector is

$$\nabla \tilde{J}(\mathbf{w}) = 2\tilde{\mathbf{B}}^{-1}(\mathbf{w} - \mathbf{w}^b) - 2\tilde{\mathbf{H}}^T \mathbf{R}^{-1}(\mathbf{y} - \tilde{\mathbf{h}}(\mathbf{w})), \quad (3.9)$$

where $\tilde{\mathbf{H}} \in \mathbb{R}^{r \times (m+q)}$ represents the linearisation of $\tilde{\mathbf{h}}$.

Proceeding as in section (2.1), we let $\mathbf{w} = \mathbf{w}^a$ at a minimum and set (3.9) to zero to yield

$$\mathbf{w}^a = \mathbf{w}^b + \tilde{\mathbf{K}}(\mathbf{y} - \tilde{\mathbf{h}}(\mathbf{w}^b)), \quad (3.10)$$

where $\tilde{\mathbf{K}} \in \mathbb{R}^{(m+q) \times r}$ is the gain matrix for the augmented system, given by

$$\tilde{\mathbf{K}} = \tilde{\mathbf{B}}\tilde{\mathbf{H}}^T \left[\tilde{\mathbf{H}}\tilde{\mathbf{B}}\tilde{\mathbf{H}}^T + \mathbf{R} \right]^{-1}. \quad (3.11)$$

If we deconstruct (3.11)

$$\begin{aligned} \tilde{\mathbf{K}} &= \begin{pmatrix} \mathbf{B}_{zz} & \mathbf{B}_{zp} \\ \mathbf{B}_{zp}^T & \mathbf{B}_{pp} \end{pmatrix} \begin{pmatrix} \mathbf{H}^T \\ \mathbf{0} \end{pmatrix} \left[\begin{pmatrix} \mathbf{H} & \mathbf{0} \end{pmatrix} \begin{pmatrix} \mathbf{B}_{zz} & \mathbf{B}_{zp} \\ \mathbf{B}_{zp}^T & \mathbf{B}_{pp} \end{pmatrix} \begin{pmatrix} \mathbf{H}^T \\ \mathbf{0} \end{pmatrix} + \mathbf{R} \right]^{-1} \\ &= \begin{pmatrix} \mathbf{B}_{zz}\mathbf{H}^T \\ \mathbf{B}_{zp}^T\mathbf{H}^T \end{pmatrix} [\mathbf{H}\mathbf{B}_{zz}\mathbf{H}^T + \mathbf{R}]^{-1} \\ &\stackrel{\text{def}}{=} \begin{pmatrix} \mathbf{K}_z \\ \mathbf{K}_p \end{pmatrix}, \end{aligned} \quad (3.12)$$

we can split the analysis equation (3.10) into state and parameter parts. This allows us to analyse

\mathbf{z}^a and \mathbf{p}^a separately as

$$\mathbf{z}^a = \mathbf{z}^b + \mathbf{K}_z(\mathbf{y} - \mathbf{h}(\mathbf{z}^b)), \quad (3.13)$$

$$\mathbf{p}^a = \mathbf{p}^b + \mathbf{K}_p(\mathbf{y} - \mathbf{h}(\mathbf{z}^b)). \quad (3.14)$$

Equation (3.13) is identical to (2.6) derived in section 2.1 and equation (3.14) for \mathbf{p}^a takes a similar form. The key difference is the presence of the cross covariance term \mathbf{B}_{zp} in the gain matrix \mathbf{K}_p .

Although the technique of state augmentation is straightforward in theory, practical implementation of the approach relies strongly on the relationships between the parameters and state components being well defined and assumes that we have sufficient knowledge to reliably describe them. Since it is not possible to observe the parameters themselves, the parameter updates are only influenced by the observations through the cross covariances that describe the correlations between the error of the model state estimate and the error of the model parameter estimate. Successful parameter estimation will therefore only be possible if these cross correlations are adequately specified. We will consider ways of defining the error covariance matrices in section 5, but first we need to introduce our model.

4 The model

We choose to start by considering a simplistic case in which the morphodynamic evolution of our system is described by the 1D linear advection model [Smith et al. (2007)],

$$\frac{\partial z}{\partial t} + a \frac{\partial z}{\partial x} = 0, \quad (4.1)$$

where $z(x, t)$ is the bathymetry or bed height, a is the advection velocity and t is the time.

As discussed in Smith et al. (2007) we can use the method of characteristics to derive an analytic solution to this equation valid at discrete points (x_i, t_k) . Given initial data

$$z(x, 0) = f(x), \quad -\infty < x < \infty, \quad (4.2)$$

the solution at time $t \geq 0$ is simply

$$z(x, t) = z(x_0, 0) = f(x - at), \quad (4.3)$$

where $x_0 = x(0)$ and $x(t) = x_0 + at$.

This represents a direct translation of the initial data. The bedform moves undistorted across the domain with constant speed a .

Since we are assuming that our parameters are fixed, the evolution model for a is given by

$$\frac{da}{dt} = 0. \quad (4.4)$$

The equation (4.4) together with the model equation (4.1) constitute our augmented state system model (3.3).

The idea is to explore the application of the state augmentation method within the framework of this simple model before moving on to a more complex model of morphodynamic evolution based on the 1D sediment conservation equation. We assume that (4.1) gives an accurate representation of the true system evolution but that the model inputs are incorrect, i.e. the advection velocity and/ or initial bathymetry are unknown. We wish to investigate whether, given an uncertain initial bathymetry and unknown advection velocity, and using observations taken from the true solution (4.3), we are able to construct an augmented data assimilation scheme that will produce a more accurate estimate of the true velocity, thereby improving the ability of our model to predict the true system state.

5 Error covariances

Error covariances play an important role in variational data assimilation. Before we can implement our 3D Var algorithm we need to define the error covariance matrices \mathbf{B} and \mathbf{R} .

We are assuming that our model is perfect, i.e. the model equations provide an exact representation of the dynamical system. Obviously, this assumption is unrealistic. In practice it is impossible to describe the true system behaviour completely. The model will also contain errors as a result of uncertain parameters and inaccurate initial and boundary conditions. In addition, the observations we wish to assimilate are likely to incorporate some kind of error, however small. Our assimilation scheme needs to take account of the errors that arise as a result of these imperfections as the precision of the analysis is determined by the precision of the background and observations. The error covariance matrices \mathbf{B} and \mathbf{R} represent our uncertainty in the background \mathbf{z}^b and observations \mathbf{y} . In order to define $\tilde{\mathbf{B}}$ for the augmented system we also need to consider the errors in the parameter estimates \mathbf{p}^b and the relationship between these errors and the errors in the background state \mathbf{z}^b . Correct specification of these matrices is crucial to the quality of the analysis. If we can ensure that these matrices are an appropriate representation of the true error statistics, our data assimilation algorithm will produce optimal results.

5.1 Observation error covariance

The observation error covariance matrix \mathbf{R} gives a statistical description of the errors in \mathbf{y} . These errors originate from instrumental error, errors in the forward model \mathbf{h} and representativeness errors [Bouttier and Courtier (2002)]. For ease of computation we assume that the observation errors are spatially and temporally uncorrelated and take \mathbf{R} to be a constant diagonal matrix with error variance σ_o^2 ,

$$\mathbf{R} = \sigma_o^2 \mathbf{I}, \quad \mathbf{I} \in \mathbb{R}^{r \times r}. \quad (5.1)$$

5.2 Background error covariance

The background error covariance matrix $\mathbf{B} = \{b_{ij}\}$ describes the estimation errors of the background state. Formulation of this matrix is one of the key parts of the assimilation problem. The correlations in \mathbf{B} govern the spreading and smoothing of observational information and are therefore fundamental in determining the nature of the resulting analysis.

Background errors arise from errors in both the initial conditions and model errors. Since, by the nature of the problem, these errors are not known exactly they have to be approximated in some manner. An approach commonly used by the NWP community is the NMC method [Parrish and Derber (1992)] which uses the difference between forecasts that verify at the same time. The literature gives various other methods for calculating \mathbf{B} , including using innovation (observation minus

background) statistics and studying differences in background fields using ensemble techniques. A review of current operational techniques is given in Fisher (2003).

Calculation of the background error covariance can be made considerably easier by specifying the error correlations as analytic functions. A number of correlation models have been proposed (see Daley (1991) for further discussion on this). One of the most simple ways of representing \mathbf{B} is to assume that the background error covariances are homogeneous and isotropic. \mathbf{B} is then equal to the estimated error variance times a correlation matrix defined using a prespecified correlation function. Although this method is somewhat crude it makes the data assimilation problem far more tractable.

5.2.1 The state vector

To characterise the background errors in the state vector \mathbf{z} we use the correlation function [Rogers (2000)]

$$b_{ij} = \sigma_b^2 \rho^{|i-j|}, \quad i, j = 1, \dots, m. \quad (5.2)$$

$\rho = \exp(-\Delta x/L)$ where Δx is the model grid spacing and L is known as the background correlation length scale.

Element b_{ij} defines the covariance between components i and j of the error vector $\boldsymbol{\varepsilon}_b$. The form (5.2) gives us a full symmetric error covariance matrix with variance σ_b^2 on the diagonal and non-zero off-diagonal elements. We can write this explicitly as

$$\mathbf{B}_{\mathbf{zz}} = \sigma_b^2 \begin{pmatrix} 1 & \rho & \rho^2 & \dots & \dots & \rho^{m-1} \\ \rho & 1 & \rho & \rho^2 & \dots & \rho^{m-2} \\ \rho^2 & \rho & 1 & \rho & \dots & \vdots \\ \vdots & \ddots & \ddots & \ddots & \ddots & \vdots \\ \vdots & & \ddots & \ddots & 1 & \rho \\ \rho^{m-1} & \dots & \dots & \rho^2 & \rho & 1 \end{pmatrix}. \quad (5.3)$$

The reason for choosing this covariance matrix is that its inverse can be calculated explicitly and has a particularly simple form (see appendix A)

$$\mathbf{B}_{\mathbf{zz}}^{-1} = \frac{\sigma_b^{-2}}{1 - \rho^2} \begin{pmatrix} 1 & -\rho & 0 & \dots & \dots & 0 \\ -\rho & 1 + \rho^2 & -\rho & 0 & & \vdots \\ 0 & -\rho & 1 + \rho^2 & -\rho & \ddots & \vdots \\ \vdots & \ddots & \ddots & \ddots & \ddots & 0 \\ \vdots & & \ddots & \ddots & 1 + \rho^2 & -\rho \\ 0 & \dots & \dots & 0 & -\rho & 1 \end{pmatrix}. \quad (5.4)$$

This makes the inversion of the augmented covariance matrix $\tilde{\mathbf{B}}$ more manageable (see appendix B).

5.2.2 The parameter vector

For the augmented system we have the added difficulty of specifying the background error covariance matrices for the parameter vector, $\mathbf{B}_{\mathbf{pp}}$, and for the cross correlations between the state and parameter errors, $\mathbf{B}_{\mathbf{zp}}$. One possible method for calculating these covariance matrices is by averaging the statistics over the assimilation window, using our knowledge of the truth and background states. However, since in reality the true solution is not known, this is difficult to do in practice. For simplicity we would like these matrices to be of a functional form similar to that used for the state background error covariance matrix, $\mathbf{B}_{\mathbf{zz}}$. Successful parameter estimation relies upon these correlations being suitably specified, so it is important to ensure that the choice of function is appropriate to the particular model application.

For our linear advection model we have a single unknown parameter - the advection velocity. We approximate the true advection velocity a with \tilde{a} where $\tilde{a} = a + \varepsilon_A$. In this case, the parameter vector \mathbf{p}^b is a scalar with error $\varepsilon_{\mathbf{p}} = \varepsilon_A$. The error covariance matrix $\mathbf{B}_{\mathbf{pp}}$ is then simply

$$E(\varepsilon_A^2) = \text{Var}(\varepsilon_A) = \sigma_A^2. \quad (5.5)$$

5.2.3 Cross covariances

To determine a suitable form for the cross covariance matrix $\mathbf{B}_{\mathbf{zp}}$ we first need to derive an expression for the background error ε_b .

We start by considering a single realisation. The background error $\varepsilon_b(x, t)$, at a particular point x and time t , will be a combination of error in the initial condition and error in the parameter estimate. We consider the following possibilities:

1. known initial state $f(x)$, known advection velocity a ;
2. unknown initial state $\tilde{f}(x)$, known advection velocity a ;
3. known initial state $f(x)$, unknown advection velocity \tilde{a} ;
4. unknown initial state $\tilde{f}(x)$, unknown advection velocity \tilde{a} .

By defining

$$\tilde{f}(x) = f(x) + \varepsilon_b^0(x), \quad (5.6)$$

and

$$\tilde{a} = a + \varepsilon_A, \quad (5.7)$$

we can derive expressions for the solution $\tilde{z}(x, t)$ and its error $\varepsilon_b(x, t)$ in each of the above cases.

Case 1: The solution is the exact solution $z(x, t)$ given by (4.3).

Case 2: Here the solution is given by

$$\tilde{z}(x, t) = \tilde{f}(x - at), \quad t \geq 0. \quad (5.8)$$

Using

$$\tilde{z}(x, t) = z(x, t) + \varepsilon_b(x, t),$$

we have

$$\varepsilon_b(x, t) = \tilde{z}(x, t) - z(x, t) = \tilde{f}(x - at) - f(x - at).$$

From (5.6)

$$\tilde{f}(x - at) = f(x - at) + \varepsilon_b^0(x - at),$$

which gives us the following expression for the error

$$\varepsilon_b(x, t) = \varepsilon_b^0(x - at) = \varepsilon_b^0(x_0). \quad (5.9)$$

In this case, the initial error profile propagates unchanged with velocity a (see figure 5.1).

Case 3: We have the solution

$$\tilde{z}(x, t) = f(x - \tilde{a}t). \quad (5.10)$$

The error at time $t \geq 0$ is

$$\begin{aligned} \varepsilon_b(x, t) &= f(x - \tilde{a}t) - f(x - at) \\ &= f(x - (a + \varepsilon_A)t) - f(x - at) \\ &= f(x - at - \varepsilon_A t) - f(x - at). \end{aligned}$$

Assuming that $f(x)$ is a continuous, differentiable function we can expand in a Taylor series about $f(x - at)$ yielding,

$$\begin{aligned} \varepsilon_b(x, t) &= f(x - at - \varepsilon_A t) - f(x - at) \\ &= \left[f(x - at) - \varepsilon_A t f'(x - at) + \frac{\varepsilon_A^2}{2!} t^2 f''(x - at) - \dots \right] - f(x - at) \\ &= -\varepsilon_A t f'(x - at) + O((\varepsilon_A t)^2) \end{aligned} \quad (5.11)$$

Solution (5.10) and its error (5.11) are illustrated in figure 5.2. Incorrect specification of the advection velocity introduces a phase error that grows with time. This error is similar in character to the derivative $f'(x)$ but increases in width and magnitude as t increases. Note that this Taylor expansion is only valid for small $\varepsilon_A t$; the approximation (5.11) breaks down as t becomes large.

Case 4: The solution at time $t \geq 0$ is

$$\tilde{z}(x, t) = \tilde{f}(x - \tilde{a}t). \quad (5.12)$$

Using Taylor series, as above, we find that the error is given by

$$\begin{aligned} \varepsilon_b(x, t) &= \tilde{f}(x - \tilde{a}t) - f(x - at) \\ &= \tilde{f}(x - at - \varepsilon_A t) - f(x - at) \\ &= \left[\tilde{f}(x - at) + \varepsilon_A t \tilde{f}'(x - at) + \frac{\varepsilon_A^2}{2!} t^2 \tilde{f}''(x - at) - \dots \right] - f(x - at) \\ &= \varepsilon_b^0(x - at) - \varepsilon_A t \tilde{f}'(x - at) + O((\varepsilon_A t)^2) \end{aligned} \quad (5.13)$$

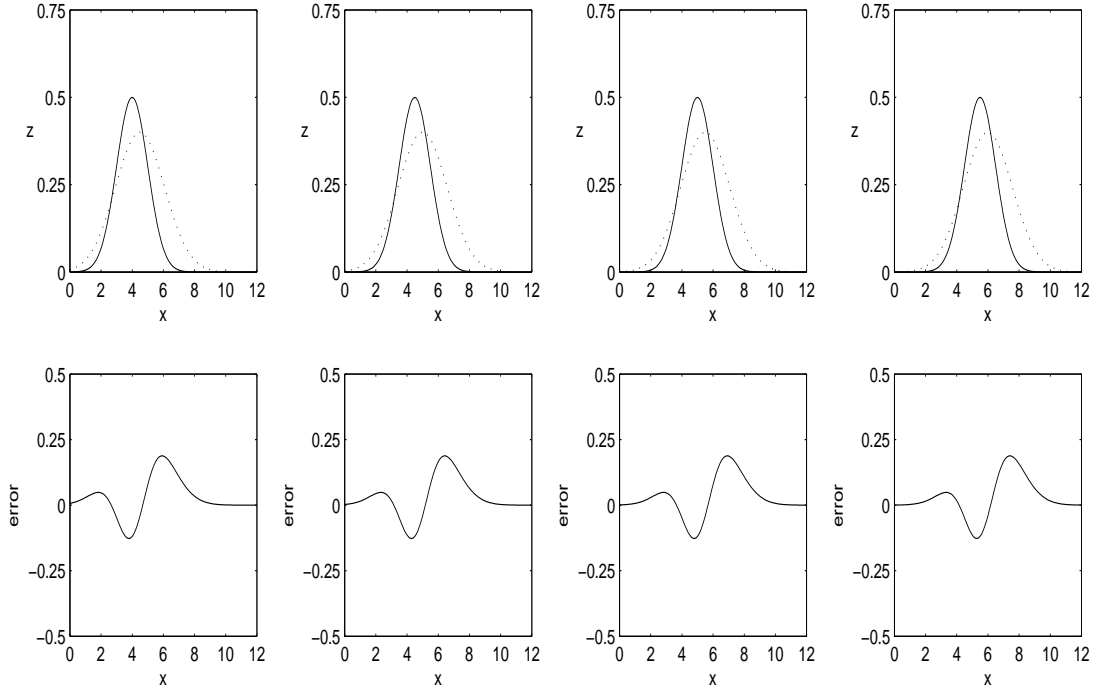


Figure 5.1: **Case 2:** unknown initial state, known advection velocity. Top: true solution $z(x, t)$ (solid line) and model solution $\tilde{z}(x, t)$ (dotted line) at times $t = 0$ to $t = 3$. Bottom: background error $\varepsilon_b(x, t)$.

If we assume that the errors $\varepsilon_b^0(x)$ are smooth we can use (5.6) to write

$$\tilde{f}'(x - at) = f'(x - at) + \varepsilon_b^0'(x - at). \quad (5.14)$$

Substituting (5.14) in to (5.13) and retaining only leading terms gives

$$\varepsilon_b(x, t) = \varepsilon_b^0(x - at) - \varepsilon_A t f'(x - at) + \dots \quad (5.15)$$

which is a combination of (5.9) and (5.11) above. As can be seen from figure 5.3, as time increases the $\varepsilon_A t f'(x - at)$ term dominates so that the errors look very similar to those in figure 5.2.

Since ε_A is scalar, the cross covariance matrix $\mathbf{B}_{z\mathbf{p}}$ will be a vector of length m . From definition (3.8) we have

$$\mathbf{B}_{z\mathbf{p}} = E(\varepsilon_b \varepsilon_{\mathbf{p}}^T) = E(\varepsilon_A \varepsilon_b) = \begin{bmatrix} E(\varepsilon_A \varepsilon_b(x_1, t)) \\ E(\varepsilon_A \varepsilon_b(x_2, t)) \\ \vdots \\ E(\varepsilon_A \varepsilon_b(x_m, t)) \end{bmatrix}. \quad (5.16)$$

Here $\varepsilon_b(x_i, t)$ is the i th component of the vector ε_b , representing the background error associated with \mathbf{z}^b at the grid point x_i at time t . Element $b_{z\mathbf{p}}(i) = E(\varepsilon_A \varepsilon_b(x_i, t))$ defines the covariance between ε_A and $\varepsilon_b(x_i, t)$. We consider two different methods for approximating these covariances.

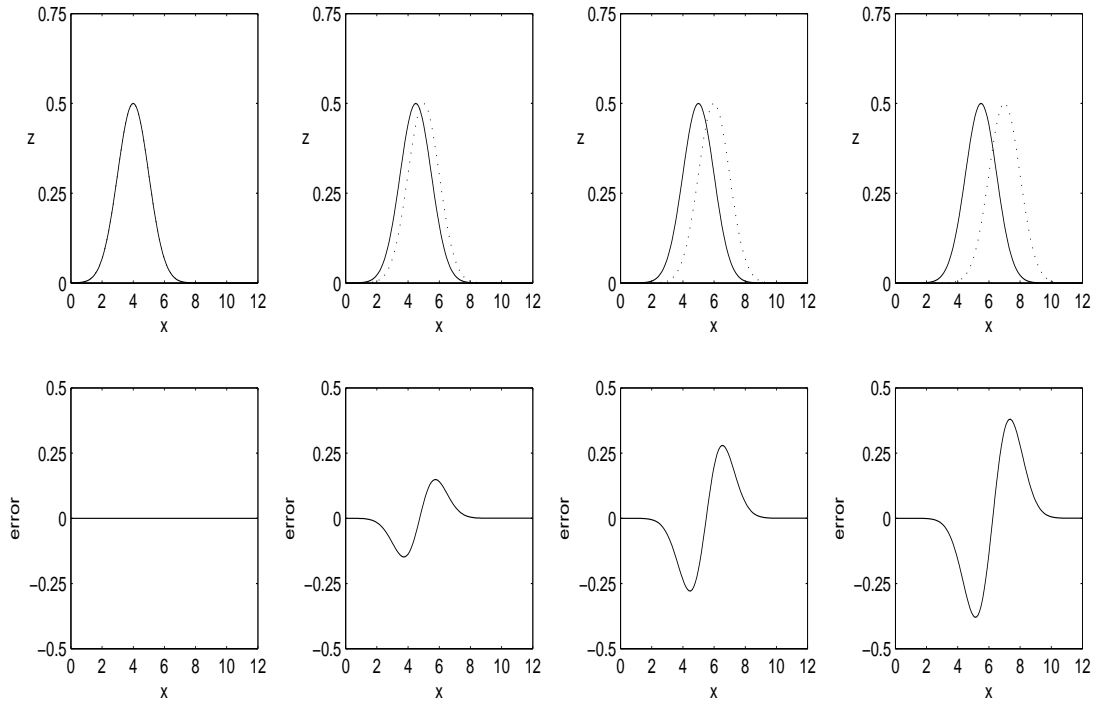


Figure 5.2: **Case 3:** known initial state, unknown advection velocity. Top: true solution $z(x, t)$ (solid line) and model solution $\tilde{z}(x, t)$ (dotted line) at times $t = 0$ to $t = 3$. Bottom: background error $\varepsilon_b(x, t)$.

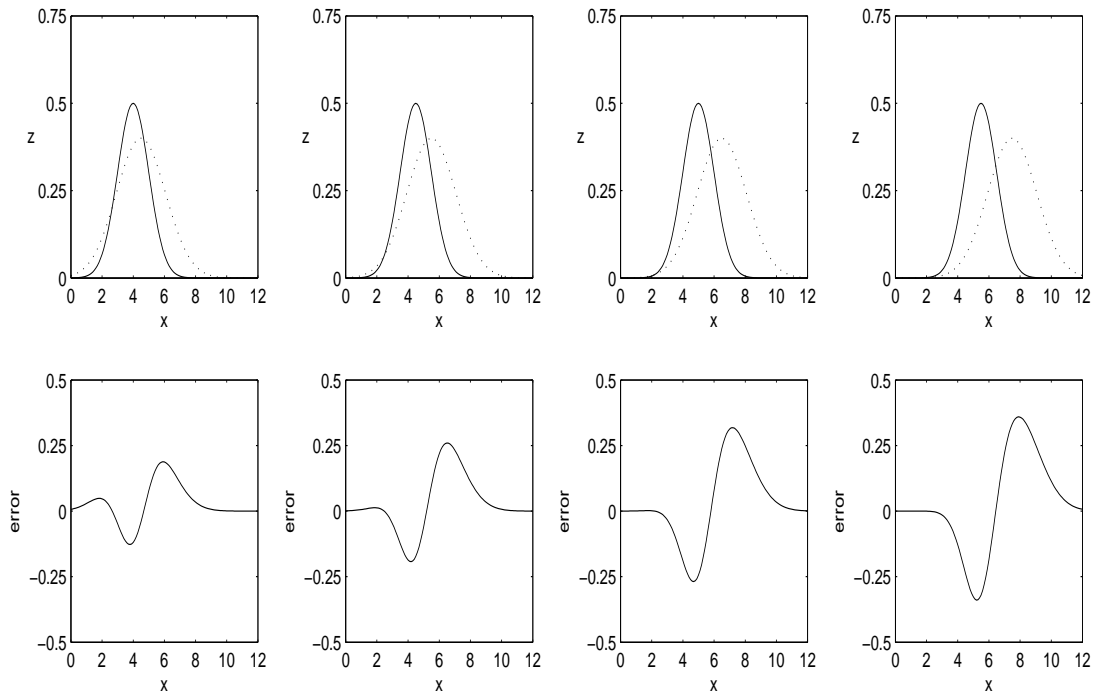


Figure 5.3: **Case 4:** unknown initial state, unknown advection velocity. Top: true solution $z(x, t)$ (solid line) and model solution $\tilde{z}(x, t)$ (dotted line) $t = 0$ to $t = 3$. Bottom: background error $\varepsilon_b(x, t)$.

Method A: The above analysis has shown that when the advection velocity a is unknown, the background error at the point x at time t is approximately proportional to $f'(x - at)t$, the value of the derivative of the initial state at the starting point x_0 multiplied by time. Conventional 3D Var schemes assume that the background error covariances are stationary and hold the matrix \mathbf{B} fixed. Since we have already made this assumption for the state background error covariance matrix \mathbf{B}_{zz} (5.3), we propose applying the same principle to the cross covariances.

Removing time dependence, we consider the following approximation to the background error,

$$\varepsilon_b(x_i) = -\tilde{\varepsilon}_A f'(x_i), \quad i = 1, \dots, m, \quad (5.17)$$

where $\tilde{\varepsilon}_A$ is an approximation of the parameter error ε_A .

Using definition (5.16), we multiply by $\tilde{\varepsilon}_A$ and take the expected value over many realisations, to give

$$\begin{aligned} b_{zp}(i) &= E(-\tilde{\varepsilon}_A^2 f'(x_i)) \\ &= -E(\tilde{\varepsilon}_A^2) f'(x_i) \\ &= -\tilde{\sigma}_A^2 f'(x_i). \end{aligned} \quad (5.18)$$

where $\tilde{\sigma}_A^2$ is the estimated parameter error variance.

Since by the nature of the problem $f'(x)$ is unknown, we approximate using our initial background estimate $\tilde{f}'(x)$ to give

$$b_{zp}(i) = -\tilde{\sigma}_A^2 \tilde{f}'(x_i), \quad i = 1, \dots, m. \quad (5.19)$$

By using (5.19) we are assuming that the matrix \mathbf{B}_{zp} is static. It's structure is determined by the derivative of the initial background bathymetry $\tilde{f}'(x)$ at t_0 and remains constant throughout the assimilation window.

Method B: The errors derived in the above example cases are based on a model with no data assimilation, and therefore assume that the form of the state approximation $\tilde{f}(x)$ and the estimated advection velocity \tilde{a} remain the same for all time. With data assimilation both the background and parameter estimates will change as the model bathymetry is updated at each new analysis time. Thus we will have a different $f(x)$ and \tilde{a} at the start of each new model integration. Matrix (5.19) used in Method A is therefore strictly only valid at a single time point. As $\tilde{f}(x)$ and \tilde{a} change, so too will their errors ε_b and ε_A . The assumption that the correlations between these errors are fixed is therefore incorrect.

We wish to take account of the fact that the background-parameter error cross covariances will change with each new analysis by reintroducing time dependency into the matrix \mathbf{B}_{zp} . Although the exact structure of the errors will vary as the data assimilation updates $\tilde{f}(x)$ and \tilde{a} , our practical experiments show that the background errors can still broadly be described by the function $f'(x - at)$. In other words, we can assume that the error at time t is approximately proportional to the initial error at the point x_0 translated to the point $x = x_0 + at$. Since both $f'(x)$ and a are unknown, we cannot evaluate $f'(x - at)$. Instead we substitute f' with \tilde{f}' and replace $(x - at)$ with $(x - \hat{\gamma})$, where $\hat{\gamma} = \hat{\gamma}(t)$ is a time dependent value that determines the speed of the error advection. The matrix \mathbf{B}_{zp} then becomes

$$b_{zp}(i) = -\tilde{\sigma}_A^2 \tilde{f}'(x_i + \hat{\gamma}(t)). \quad (5.20)$$

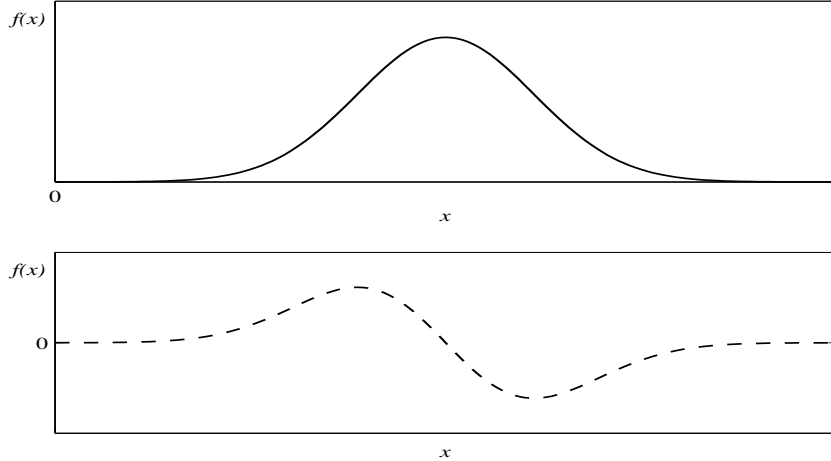


Figure 6.1: initial data (solid line) and its derivative (dashed line).

$\hat{\gamma}(t)$ is updated at each new analysis time and is chosen so that the error profile $\tilde{f}'(x - \hat{\gamma})$ is centred on the point at which the background solution takes its maximum value.

6 The experiments

We assume that the morphodynamic evolution of the true system is described by the linear advection model (4.1) with an initial bathymetry given by the Gaussian exponential function

$$z(x, 0) = f(x) = \alpha e^{-\beta(x-\gamma)^2}, \quad (6.1)$$

so that

$$f'(x) = -2\alpha\beta(x - \gamma)e^{-\beta(x-\gamma)^2}, \quad (6.2)$$

This gives us a smooth bell-shaped bed form (see figure 6.1). Here, α , β and γ are arbitrary constants whose values determine the height, width and position of the curve respectively.

Given an approximate velocity \tilde{a} and starting from a perturbed initial state we wish to examine whether our augmented scheme is able to deliver both an accurate model bathymetry *and* an accurate estimate of the true advection velocity a . The quality of the analysis will be evaluated against the true solution (4.3).

For the purpose of these experiments we set the true advection velocity $a = 0.5$. The background state at t_0 was taken to be of the same form as the true initial bathymetry (6.1) but with perturbed values of α , β and γ . The assimilation algorithm is applied sequentially as described in section 2.2 with observations being assimilated every N timesteps, where the value of N is specified by the user. At each new analysis phase a set of observations are generated; they are used only once, at the correct time, and not again. The cost function is minimised iteratively using a Quasi-Newton descent algorithm [Gill et al. (1981)].

For ease of computation, observations are taken from the true solution and at points that coincide with the model grid. We set

$$y_i = z_i^t,$$

where y_i is an observation of the true bathymetry z_i^t given by (4.3) at the grid point x_i . The observation operator \mathbf{h} is linear and $\mathbf{h} = \mathbf{H}$. The matrix $\mathbf{H} \in \mathbb{R}^{r \times m}$ takes a very simple form; it consists almost entirely of zeros except at positions corresponding to an observation location which take a value of one. The observation locations are determined at the start of the assimilation and remain fixed throughout. Since the observations are drawn from the truth we weight in their favour, setting the observation and background error variances to be $\sigma_o^2 = 0.1$ and $\sigma_b^2 = 1.0$ respectively.

The observation error covariance matrix \mathbf{R} and sub-matrices \mathbf{B}_{zz} , \mathbf{B}_{pp} of the augmented background error covariance matrix $\tilde{\mathbf{B}}$ were defined using (5.1), (5.3) and (5.5) respectively. Experiments were run using both method A (5.19) and B (5.20) to approximate the cross covariance matrix \mathbf{B}_{zp} . Results are presented in the following section.

7 Results

Figures 7.2 and 7.3 show the analysis produced for method A with initial parameter estimates (a) $\tilde{a} = 0.25$ and (b) $\tilde{a} = 0.75$. Results are given for times $t = 0$ to 20 with time step $\Delta t = 0.1$. Observations were taken at $20\Delta x$ intervals and assimilated every 20 time steps (2 time units). The dotted line represents the true bathymetry \mathbf{z}^t . Observations \mathbf{y} are given by circles, the background \mathbf{z}^b by the dashed line and the analysis \mathbf{z}^a by the solid line. We found that although qualitatively the analysis is close to the truth (the main differences being small phase and amplitude errors), the scheme was unable to recover the true value of a . The parameter updates are shown in figure 7.1; the estimates do converge but to incorrect values of 0.379 and 0.799 respectively. In both cases we reach a point at around $t = 10$ after which the assimilation of new observations has no effect. We conclude that the representation of the cross covariances used in method A is inadequate.

The evolution of the parameter estimates using method B is shown in figures 7.5 to 7.8 for observations taken at (a) $10\Delta x$ (b) $20\Delta x$ and (c) $40\Delta x$ intervals and assimilated every 10 and 20 time steps. The accuracy of the estimated advection velocity increases with time as the assimilation cycle is repeated and more observations are processed. The scheme converges in all cases, managing to successfully recover the true value of a with a final value of 0.50 to 2 d.p. As a result the model becomes a much better approximation and thus produces more accurate estimates of the true bathymetry as is illustrated in figure 7.4 for the case $\tilde{a} = 0.75$. After 100 time steps ($t = 10$) it is almost impossible to distinguish between the predicted model bathymetry and the truth.

The experiments were repeated for a range of starting values and observation combinations. The speed of convergence varies depending on the initial background guess, the location and spatial frequency of the observations and the time between successive assimilations. Although there is little difference in the speed of convergence for observations taken at intervals of $10\Delta x$ and $20\Delta x$, the scheme takes more than twice as long to reach the true a value when the spatial frequency of the observations is halved again to every $40\Delta x$. Comparing figures 7.5 and 7.6, and 7.7 and 7.8 we see that there are only small differences in the convergence when the time between assimilations is increased from every 10 to every 20 time steps. However, as the time between successive assimilations is increased further the rate of convergence slows considerably. Generally, we found that the lower the spatial and temporal frequency of the observations the longer the scheme takes to reach the correct a value. The quality of the analysis is also affected. If the observations become too infrequent the parameter estimates fail to converge. This raises the issue of observability; whether the available observations contain sufficient information for us to be able to reconstruct the model state. We will not discuss the concept any further here but note that it is a question that will need to be addressed in future work.

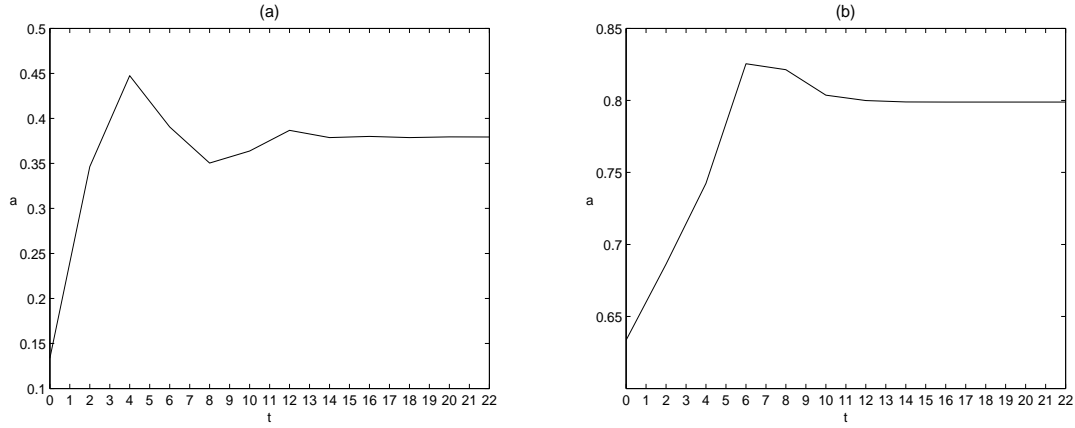


Figure 7.1: Convergence with fixed matrix $\tilde{\mathbf{B}}$ (a) $\tilde{a} = 0.25$ (b) $\tilde{a} = 0.75$. with timestep $\Delta t = 0.1$ and grid spacing $\Delta x = 0.1$. Observations taken at $20\Delta x$ intervals and assimilated every 2 time units

8 Conclusions

This work is motivated by the problem of parameter estimation in morphodynamic modelling. In this report, we have presented a novel approach using data assimilation. By employing the technique of state augmentation we have constructed a scheme that has been shown to be capable of recovering near-perfect parameter values and therefore improving the ability of our model to predict future bathymetry. To date the technique has only been developed and tested in a simplified 1D single parameter model. The results are promising and indicate that there is great potential for the use of data assimilation based parameter estimation.

Quality of the analysis is highly dependent on the accuracy of the information we feed into the assimilation algorithm. In the above experiments, we assumed perfect observations drawn from the true solution. We weighted heavily in their favour because we were confident of their accuracy. In reality, observational data are noisy and distributed unevenly in space and time. One way of simulating such errors is to add random noise to the observations. This would then allow us to examine the extent to which over/ under estimation of observation error affects our results.

The key issue that this study has highlighted is the importance of the correct specification of the covariances between the background and parameter errors. As the numerical experiments of section 7 have shown, in order to yield accurate approximations of both the bathymetry and the model parameters, we must ensure that these correlations are well defined. In this work we have relied heavily on our a priori knowledge of the parameter and of the behaviour of the solution, but in practice we may not have this type of information. Future studies should perhaps give more consideration to this.

The long term aim of this work is to implement the scheme in a full morphodynamic assimilation-forecast system. The next step in this process is to try and reproduce the success of the linear model in a less simplistic non-linear model that has two uncertain parameters. This will offer further challenges since in addition to the correlations between state and parameter errors we will also need to consider the correlations between parameters and the possibility of non-uniqueness of solutions. This is where the parameters do not converge to a single deterministic set of values, but rather there exists a range of complementary combinations that produce the same model behaviour.

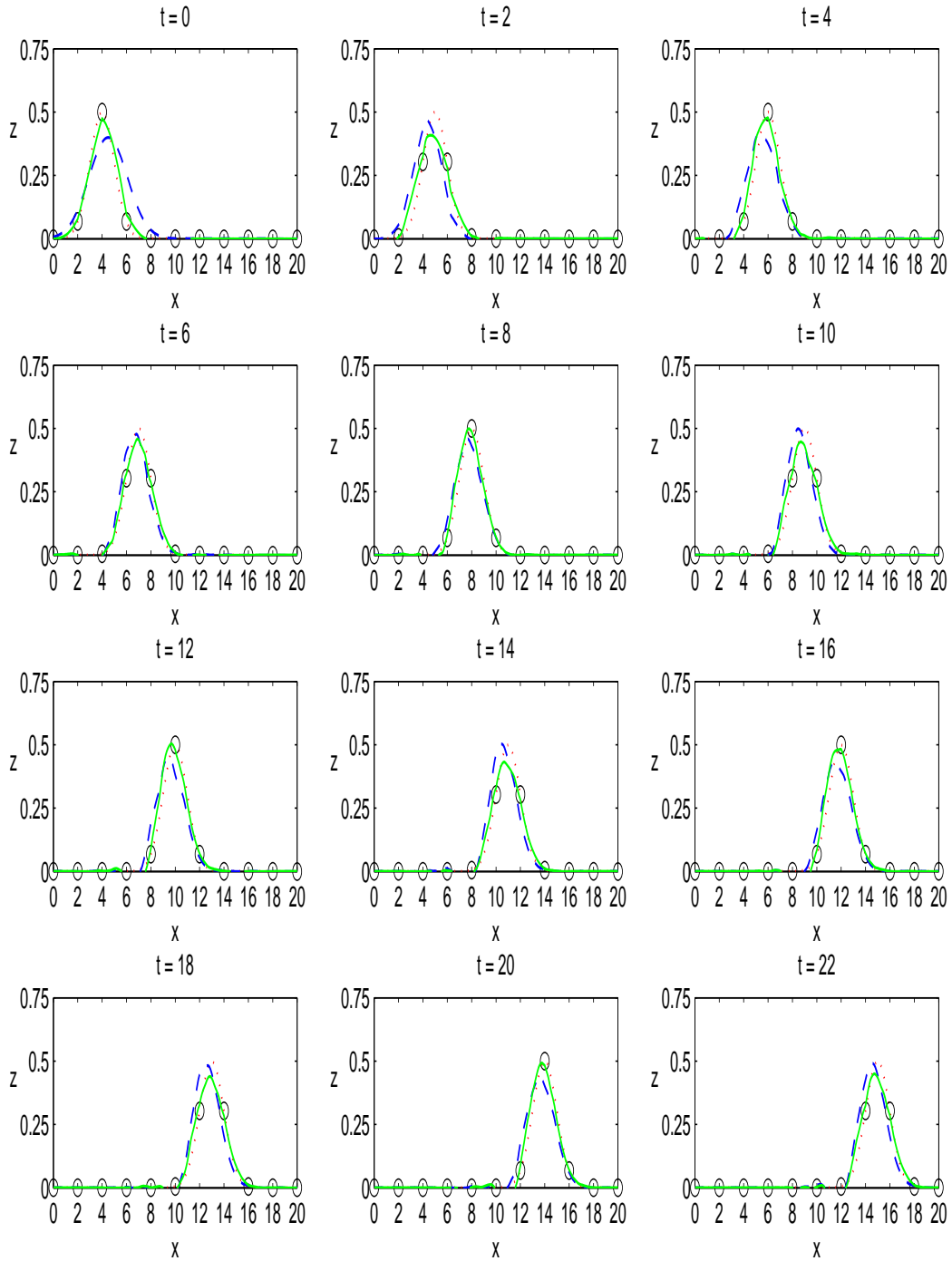


Figure 7.2: Analysis with fixed matrix $\tilde{\mathbf{B}}$: $\tilde{a} = 0.25$ with timestep $\Delta t = 0.1$ and grid spacing $\Delta x = 0.1$. Observations taken at $20\Delta x$ intervals and assimilated every 2 time units. The dotted line represents the true bathymetry \mathbf{z}^t . Observations \mathbf{y} are given by circles, the background \mathbf{z}^b by the dashed line and the analysis \mathbf{z}^a by the solid line.

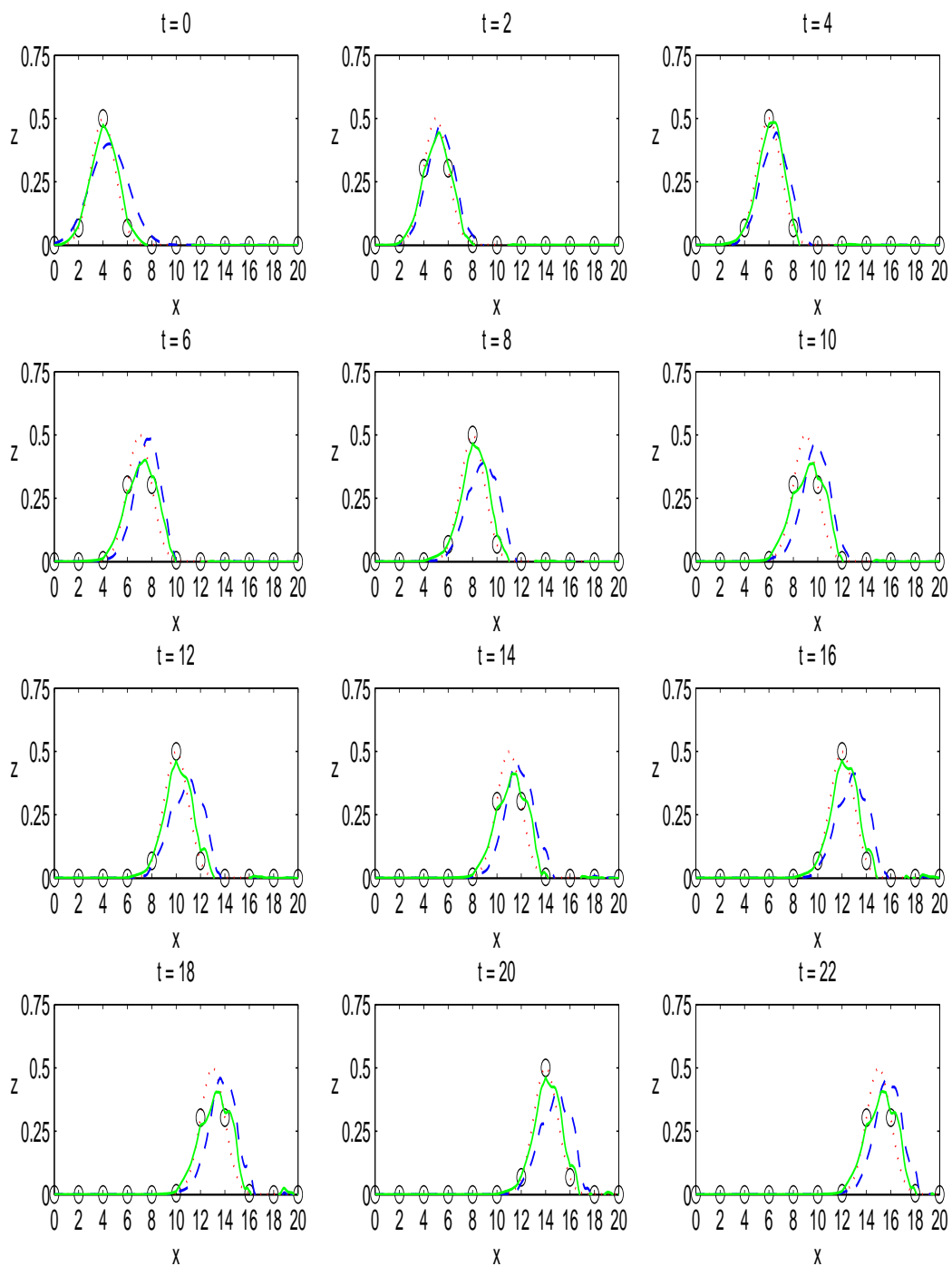


Figure 7.3: Analysis with fixed matrix $\tilde{\mathbf{B}}$: $\tilde{a} = 0.75$ with timestep $\Delta t = 0.1$ and grid spacing $\Delta x = 0.1$. Observations taken at $20\Delta x$ intervals and assimilated every 2 time units. The dotted line represents the true bathymetry \mathbf{z}^t . Observations \mathbf{y} are given by circles, the background \mathbf{z}^b by the dashed line and the analysis \mathbf{z}^a by the solid line.

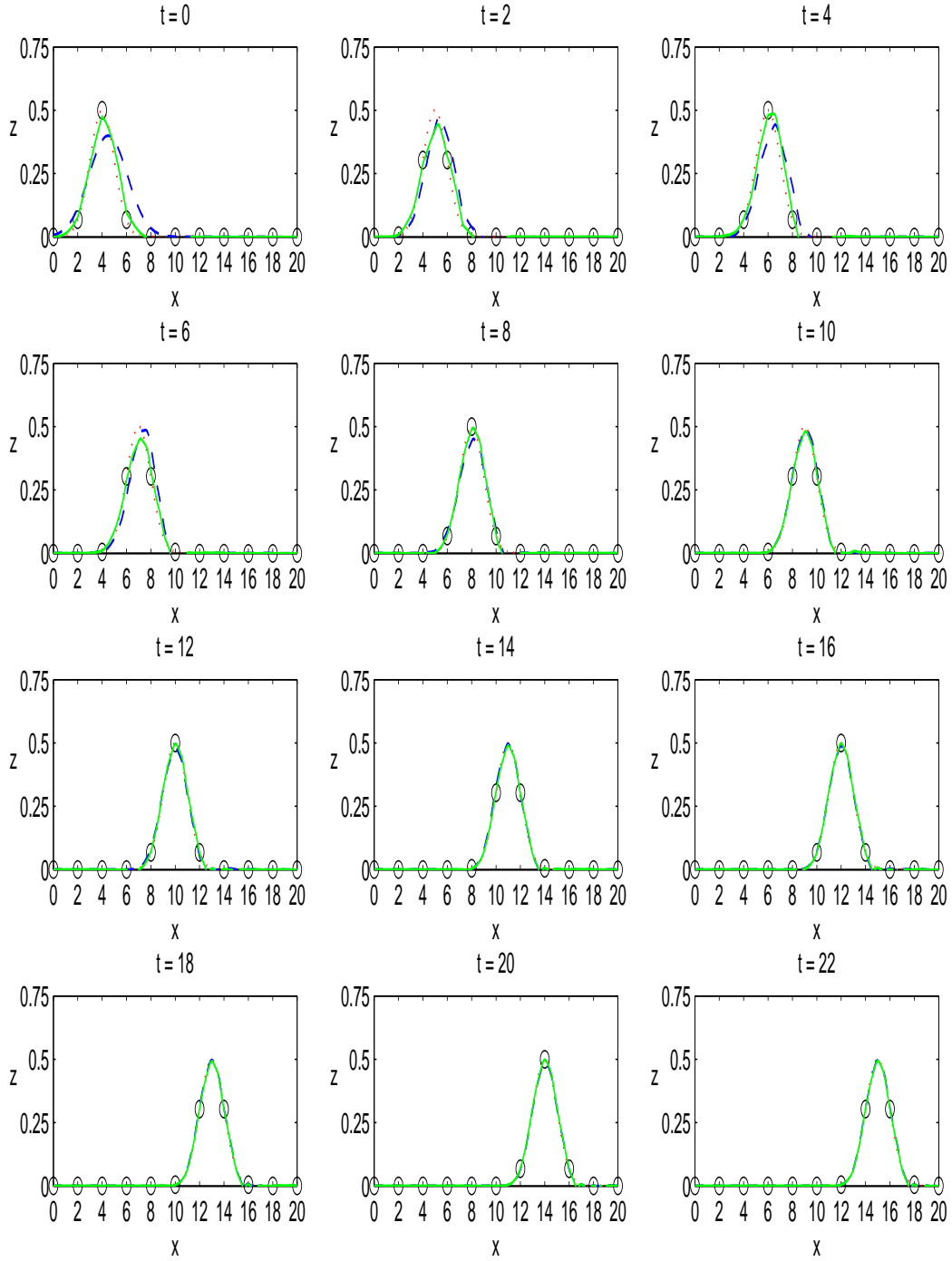


Figure 7.4: Analysis with time varying cross covariance matrix \mathbf{B}_{zp} : $\tilde{a} = 0.75$ with time step $\Delta t = 0.1$ and grid spacing $\Delta x = 0.1$. Observations taken at $20\Delta x$ intervals and assimilated every 2 time units. The dotted line represents the true bathymetry \mathbf{z}^t . Observations \mathbf{y} are given by circles, the background \mathbf{z}^b by the dashed line and the analysis \mathbf{z}^a by the solid line.

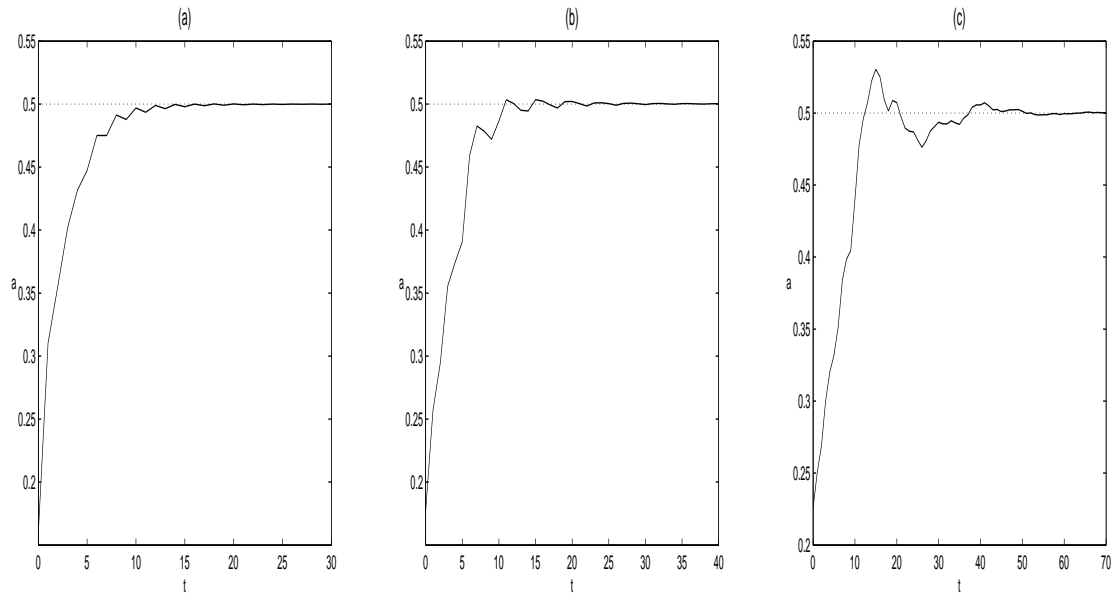


Figure 7.5: Convergence with time varying cross covariance matrix \mathbf{B}_{zp} : $\tilde{a} = 0.25$ with time step $\Delta t = 0.1$ and grid spacing $\Delta x = 0.1$. Observations taken at (a) $10\Delta x$, (b) $20\Delta x$, (c) $40\Delta x$ intervals and assimilated every 1 time unit.

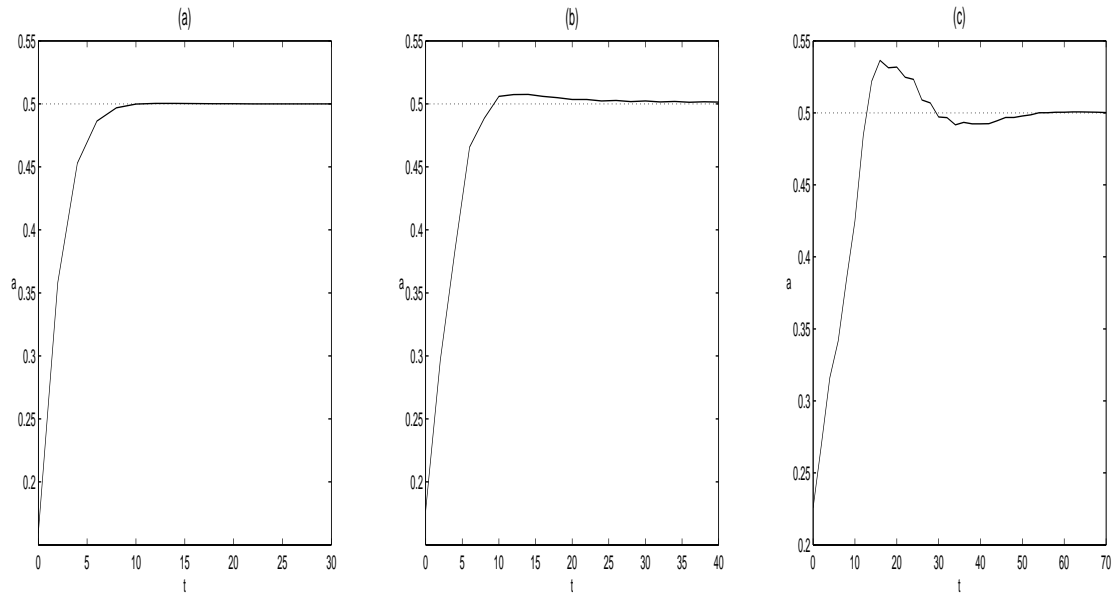


Figure 7.6: Convergence with time varying cross covariance matrix \mathbf{B}_{zp} : $\tilde{a} = 0.25$ with time step $\Delta t = 0.1$ and grid spacing $\Delta x = 0.1$. Observations taken at (a) $10\Delta x$, (b) $20\Delta x$, (c) $40\Delta x$ intervals and assimilated every 2 time units.

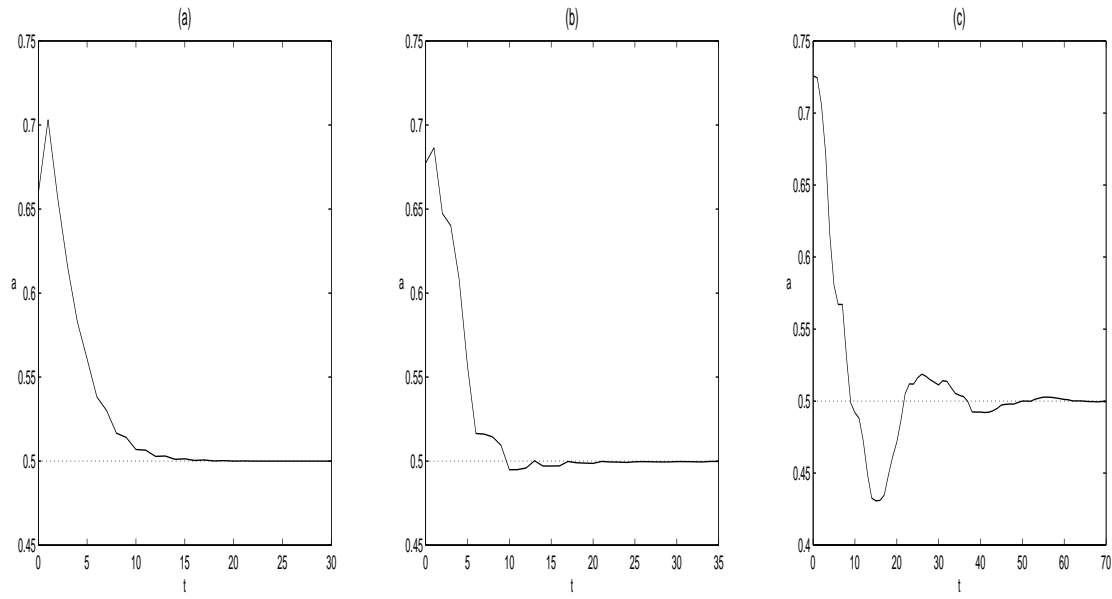


Figure 7.7: Convergence with time varying cross covariance matrix \mathbf{B}_{zp} : $\tilde{a} = 0.75$ with time step $\Delta t = 0.1$ and grid spacing $\Delta x = 0.1$. Observations taken at (a) $10\Delta x$, (b) $20\Delta x$, (c) $40\Delta x$ intervals and assimilated every 1 time unit.

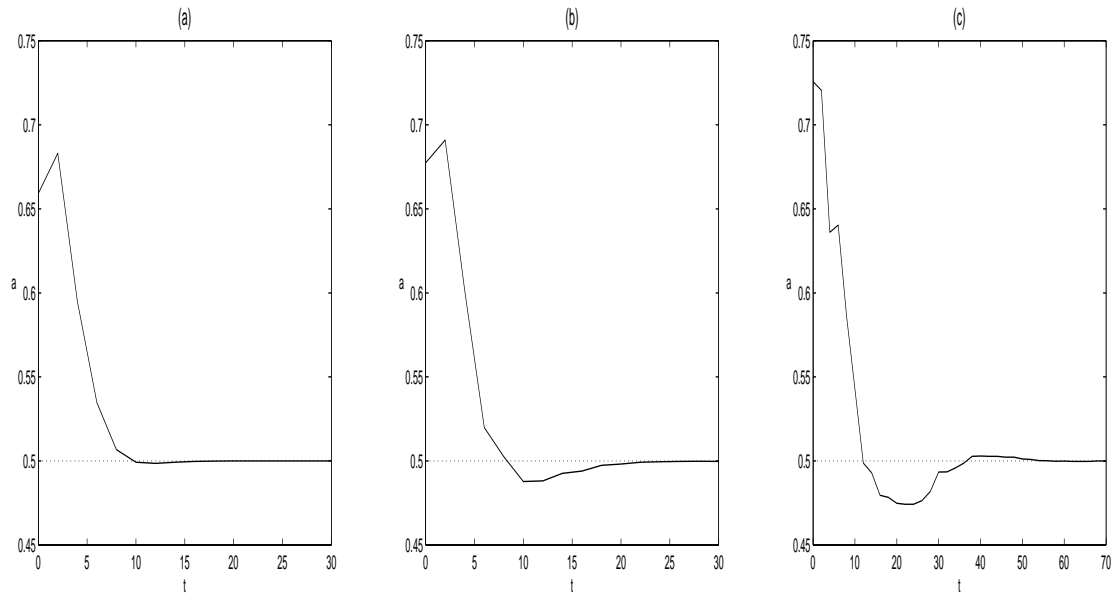


Figure 7.8: Convergence with time varying cross covariance matrix \mathbf{B}_{zp} : $\tilde{a} = 0.75$ with time step $\Delta t = 0.1$ and grid spacing $\Delta x = 0.1$. Observations taken at (a) $10\Delta x$, (b) $20\Delta x$, (c) $40\Delta x$ intervals and assimilated every 2 time units.

Appendices

A Inverting matrix \mathbf{B}

By factorising \mathbf{B} into the form $\mathbf{B} = \mathbf{L}\mathbf{D}\mathbf{L}^T$ where \mathbf{L} is a lower diagonal matrix

$$\mathbf{L} = \begin{pmatrix} 1 & 0 & \cdots & \cdots & \cdots & 0 \\ \rho & 1 & 0 & \cdots & \cdots & \vdots \\ \rho^2 & \rho & 1 & 0 & \cdots & \vdots \\ \vdots & \ddots & \ddots & \ddots & \ddots & \vdots \\ \vdots & & & \ddots & \ddots & 1 & 0 \\ \rho^{m-1} & \cdots & \cdots & \rho^2 & \rho & 1 \end{pmatrix},$$

and \mathbf{D} is the diagonal matrix

$$\mathbf{D} = \sigma_b^2 \begin{pmatrix} 1 & 0 & \cdots & \cdots & 0 \\ 0 & (1-\rho^2) & 0 & \cdots & \vdots \\ \vdots & 0 & (1-\rho^2) & & \vdots \\ \vdots & & & \ddots & \vdots \\ 0 & \cdots & \cdots & \cdots & (1-\rho^2) \end{pmatrix},$$

we can write its inverse as $\mathbf{B}^{-1} = (\mathbf{L}\mathbf{D}\mathbf{L}^T)^{-1} = \mathbf{L}^{-T}\mathbf{D}^{-1}\mathbf{L}^{-1}$, where

$$\mathbf{L}^{-1} = \begin{pmatrix} 1 & 0 & \cdots & \cdots & 0 \\ -\rho & 1 & 0 & & \vdots \\ 0 & \ddots & \ddots & \ddots & \vdots \\ \vdots & \ddots & \ddots & 1 & 0 \\ 0 & \cdots & 0 & -\rho & 1 \end{pmatrix},$$

and

$$\mathbf{D}^{-1} = \frac{\sigma_b^{-2}}{1-\rho^2} \begin{pmatrix} 1-\rho^2 & 0 & \cdots & \cdots & 0 \\ 0 & 1 & 0 & & \vdots \\ \vdots & \ddots & \ddots & \ddots & \vdots \\ \vdots & & & \ddots & 1 & 0 \\ 0 & \cdots & \cdots & 0 & 1 \end{pmatrix}.$$

This gives us a tridiagonal matrix of the form

$$\mathbf{B}^{-1} = \frac{\sigma_b^{-2}}{1 - \rho^2} \begin{pmatrix} 1 & -\rho & 0 & \cdots & \cdots & 0 \\ -\rho & 1 + \rho^2 & -\rho & 0 & & \vdots \\ 0 & -\rho & 1 + \rho^2 & -\rho & \ddots & \vdots \\ \vdots & \ddots & \ddots & \ddots & \ddots & 0 \\ \vdots & & & & & \\ 0 & \cdots & \cdots & 0 & -\rho & 1 \end{pmatrix}. \quad (\text{A.1})$$

B Block Matrix Inversion

If we partition the augmented background error covariance matrix $\tilde{\mathbf{B}}$ into block form

$$\tilde{\mathbf{B}} = \begin{pmatrix} \mathbf{B}_{zz} & \mathbf{B}_{zp} \\ \mathbf{B}_{pz} & \mathbf{B}_{pp} \end{pmatrix}, \quad (\text{B.1})$$

we can invert $\tilde{\mathbf{B}}$ blockwise using the analytic inversion formula:

$$\begin{aligned} \tilde{\mathbf{B}}^{-1} &= \begin{pmatrix} \mathbf{B}_{zz} & \mathbf{B}_{zp} \\ \mathbf{B}_{pz} & \mathbf{B}_{pp} \end{pmatrix}^{-1} \\ &= \begin{pmatrix} \mathbf{B}_{zz}^{-1} + \mathbf{B}_{zz}^{-1} \mathbf{B}_{zp} (\mathbf{B}_{pp} - \mathbf{B}_{pz} \mathbf{B}_{zz}^{-1} \mathbf{B}_{zp})^{-1} \mathbf{B}_{pz} \mathbf{B}_{zz}^{-1} & -\mathbf{B}_{zz}^{-1} \mathbf{B}_{zp} (\mathbf{B}_{pp} - \mathbf{B}_{pz} \mathbf{B}_{zz}^{-1} \mathbf{B}_{zp})^{-1} \\ -(\mathbf{B}_{pp} - \mathbf{B}_{pz} \mathbf{B}_{zz}^{-1} \mathbf{B}_{zp})^{-1} \mathbf{B}_{pz} \mathbf{B}_{zz}^{-1} & (\mathbf{B}_{pp} - \mathbf{B}_{pz} \mathbf{B}_{zz}^{-1} \mathbf{B}_{zp})^{-1} \end{pmatrix}. \end{aligned} \quad (\text{B.2})$$

Alternatively this can be written as

$$\tilde{\mathbf{B}}^{-1} = \begin{pmatrix} (\mathbf{B}_{zz} - \mathbf{B}_{zp} \mathbf{B}_{pp}^{-1} \mathbf{B}_{pz})^{-1} & -(\mathbf{B}_{zz} - \mathbf{B}_{zp} \mathbf{B}_{pp}^{-1} \mathbf{B}_{pz})^{-1} \mathbf{B}_{zp} \mathbf{B}_{pp}^{-1} \\ -\mathbf{B}_{pp}^{-1} \mathbf{B}_{pz} (\mathbf{B}_{zz} - \mathbf{B}_{zp} \mathbf{B}_{pp}^{-1} \mathbf{B}_{pz})^{-1} & \mathbf{B}_{pp}^{-1} + \mathbf{B}_{pp}^{-1} \mathbf{B}_{pz} (\mathbf{B}_{zz} - \mathbf{B}_{zp} \mathbf{B}_{pp}^{-1} \mathbf{B}_{pz})^{-1} \mathbf{B}_{zp} \mathbf{B}_{pp}^{-1} \end{pmatrix}. \quad (\text{B.3})$$

By the matrix inversion lemma [Petersen and Pedersen (2008)] we can equate (B.2) and (B.3)

$$(\mathbf{B}_{zz} - \mathbf{B}_{zp} \mathbf{B}_{pp}^{-1} \mathbf{B}_{pz})^{-1} = \mathbf{B}_{zz}^{-1} + \mathbf{B}_{zz}^{-1} \mathbf{B}_{zp} (\mathbf{B}_{pp} - \mathbf{B}_{pz} \mathbf{B}_{zz}^{-1} \mathbf{B}_{zp})^{-1} \mathbf{B}_{pz} \mathbf{B}_{zz}^{-1}$$

we get

$$\tilde{\mathbf{B}}^{-1} = \begin{pmatrix} (\mathbf{B}_{zz} - \mathbf{B}_{zp} \mathbf{B}_{pp}^{-1} \mathbf{B}_{pz})^{-1} & -(\mathbf{B}_{zz} - \mathbf{B}_{zp} \mathbf{B}_{pp}^{-1} \mathbf{B}_{pz})^{-1} \mathbf{B}_{zp} \mathbf{B}_{pp}^{-1} \\ -\mathbf{B}_{pp}^{-1} \mathbf{B}_{pz} (\mathbf{B}_{zz} - \mathbf{B}_{zp} \mathbf{B}_{pp}^{-1} \mathbf{B}_{pz})^{-1} & (\mathbf{B}_{pp} - \mathbf{B}_{pz} \mathbf{B}_{zz}^{-1} \mathbf{B}_{zp})^{-1} \end{pmatrix}. \quad (\text{B.4})$$

We find that (B.4) gives better Matlab matrix conditioning and so we use this form in our work.

References

- Bouttier, F. and Courtier, P. (2002). Data assimilation concepts and methods. Meteorological Training Course Lecture Series. ECMWF.
- Daley, R. (1991). *Atmospheric Data Analysis*. Cambridge University Press.
- Dee, D. P. (2005). Bias and data assimilation. *Quarterly Journal of the Royal Meteorological Society*, 131:3323–2243.
- Evensen, G., Dee, D. P., and Schröter, J. (1998). Parameter estimation in dynamical models. In Chassignet, E. and Verron, J., editors, *Ocean Modeling and Parameterization*, pages 373–398. Kluwer Academic Publishers.
- Fisher, M. (2003). Background error covariance modelling. In *Seminar on recent developments in data assimilation for atmosphere and ocean*, pages 49–64. ECMWF.
- Gill, P. E., Murray, W., and Wright, M. H. (1981). *Practical Optimization*. Academic Press.
- Griffith, A. K. (1997). *Data Assimilation for Numerical Weather Prediction Using Control Theory*. PhD thesis, University of Reading.
- Griffith, A. K. and Nichols, N. K. (1996). Accounting for model error in data assimilation using adjoint methods. In Berz, M., Bischof, C., Corliss, G., and Griewank, A., editors, *Computational Differentiation: Techniques, Applications and Tools*, pages 195–204. SIAM Philadelphia.
- Jazwinski, A. H. (1970). *Stochastic Processes and Filtering Theory*. Academic Press.
- Kalnay, E. (2003). *Atmospheric Modeling, Data Assimilation and Predictability*. Cambridge University Press.
- Lesser, G., Roelvink, J., van Kester, J., and Stelling, G. (2004). Development and validation of a three-dimensional morphological model. *Coastal Engineering*, 51:883–915.
- Martin, M. J. (2000). *Data Assimilation in Ocean Circulation Models with Systematic Errors*. PhD thesis, University of Reading.
- Masselink, G. and Hughes, M. G. (2003). *Introduction to Coastal Processes and Geomorphology*. Hodder Arnold.
- Navon, I. M. (1997). Practical and theoretical aspects of adjoint parameter estimation and identifiability in meteorology and oceanography. *Dynamics of Atmosphere and Oceans*, 27:55–79.
- Nicholls, R., Wong, P., Burkett, V., Codignotto, J., Hay, J., McLean, R., Ragoonaden, S., and Woodroffe, C. (2007). Chapter 6: Coastal systems and low-lying areas. In *Climate Change 2007: Impacts, Adaptation and Vulnerability. Contribution of Working Group II to the Fourth Assessment Report of the Intergovernmental Panel on Climate Change*, pages 315–356. Cambridge University Press.
- Nichols, N. K. (2003). Data assimilation: Aims and basic concepts. In Swinbank, R., Shutyaev, V., and Lahoz, W., editors, *Data Assimilation for the Earth System*, volume 26 of *Nato Science Series IV: Earth & Environmental Sciences*, pages 9–20. Kluwer Academic.
- Parrish, D. F. and Derber, J. C. (1992). The national meteorological center’s spectral statistical-interpolation analysis system. *Monthly Weather Review*, 120:1747–1763.

- Petersen, K. B. and Pedersen, M. S. (2008). *The Matrix Cookbook*. Technical University of Denmark.
URL: <http://matrixcookbook.com/>.
- Rodgers, C. D. (2000). *Inverse Methods for Atmospheric Sounding: Theory and Practice*, volume 2 of *Series on Atmospheric, Oceanic and Planetary Physics*. World Scientific.
- Scott, T. R. and Mason, D. C. (2007). Data assimilation for a coastal area morphodynamic model: Morecambe bay. *Coastal Engineering*, 54:91–109.
- Smith, P. J., Baines, M. J., Dance, S. L., Nichols, N. K., and Scott, T. R. (2007). Simple models of changing bathymetry with data assimilation. Numerical Analysis Report 10/2007, Department of Mathematics, Univeristy of Reading.
- Stelling, G. (2000). A numerical method for inundation simulations. In Yoon, Y., Jun, B., Seoh, B., and Choi, G., editors, *Proc. 4th International Conference on Hydro-Science and Engineering, Seoul, Korea*.